Short communication

Visualization of electrolyte volatile phenomenon in DIR-MCFC

Kimihiko Sugiura [a,*], Tadakatsu Yodo [a], Makoto Yamauchi [a], Kazumi Tanimoto [b]

[a] *Osaka Prefectural College of Technology, 26-12 Saiwai, Neyagawa, Osaka 572-8572, Japan*
[b] *National Institutes of Advanced Industrial Science and Technology, Kansai 1-8-31, Midorigaoka, Ikeda, Osaka 563-8577, Japan*

Abstract

Volatilization of molten salt is one of the factors that control the performance of molten carbonate fuel cells (MCFC). Volatilization of molten salt promotes cross-leakage and the corrosion of metallic components. Moreover, piping blockage is caused by the solidification of volatile matter. Because reforming catalysts filling the anode channel are polluted by molten salt volatile matter in direct internal reforming molten carbonate fuel cells (DIR-MCFC), the volatilization of molten salt is an especially serious subject. However, neither the behaviour nor the volatilization volume of molten salt volatile matter has heretofore been elucidated on. Because molten salt volatile matter that has strong alkalinity cannot be supplied directly to an analyzer, its volatilization volume is small, and analytical accuracy is poor. Therefore, an attempt has been made to elucidate about the electrolyte volatile phenomenon in an MCFC by using a non-contact image measurement technique. A 16 cm^2 MCFC single cell frame has an observation window and an irradiation window. The image of the volatile phenomenon is shown by irradiating a YAG laser light sheet 2 mm thick from an irradiation window into the anode channel, and taking measurements from an observation window with a high spatial resolution video camera (12 bit). As a result, though the volatile matter is not observed in an anode channel at OCV, the volatile matter flows in a belt-like manner from the inlet side near the electrode toward the outlet at a current density of 150 mA cm^{-2}. In addition, volatile matter is difficult to observe with the conventional thickness of an anode electrode. Because the composition of these volatile matters is $15Li_2CO_3/85K_2CO_3$ (the result of conversion into molten salt) by ion chromatography analysis, it is not an electrolyte ($62Li_2CO_3/38K_2CO_3$) but rather the volatile matter of potassium, such as KOH. Therefore, it is understood that the volatile matter K_2CO_3 is generated as KOH, comprising the water generated by the cellular reaction with an electrolyte, in a reaction with CO_2. Conversely, the volatile matter flows to the surface of the cathode electrode without regard to changes in current density. In addition, the volatile matter exists on the electrode surface, although it decreases more or less with the conventional thickness of the cathode electrode. Therefore, it is understood that the volatile matter, in order for it not to be related to the cellular reaction, does not comprise the dispersion of molten salt.
© 2006 Elsevier B.V. All rights reserved.

Keywords: MCFC; Volatilizing molten carbonate; Vapour-phase pollution; Visualization; Image measurement technique

1. Introduction

Direct internal reforming molten carbonate fuel cells (DIR-MCFC) have high-energy efficiency, because the hydrogen generated by the reforming reaction at the anode channel is used for the cell reaction. Moreover, DIR-MCFC decreases the amount of the steam supply by using the water generated by a cell reaction to reform the reaction. However, in direct internal reforming molten carbonate fuel cells (DIR-MCFC), the deterioration of catalytic activity takes place in the anode channel due to both the liquid-phase pollution and the vapour-phase pollution [1]. Liquid-phase pollution means that catalytic activity is deteriorated by molten salts ($62Li_2CO_3/38K_2CO_3$ or $52Li_2CO_3/48Na_2CO_3$) adhering to the catalyst [2], a problem, which can be solved by installing a protective barrier in the pollutant pathway [3]. Conversely, we are convinced that vapour-phase pollution is catalytic activity, which is deteriorated by KOH (or NaOH) adhering to the catalyst [4]. Moreover, last year we elucidated the amount of volatilized hydroxide by a non-contact image measurement technique, and have observed the volatile matter in the anode channel [5]. Therefore, we will attempt visualization of the volatile phenomenon in both electrodes to elucidate on the electrolyte volatile phenomenon in MCFC by a non-contact image measurement technique. The

---

16 cm^2 MCFC single cell' frame has an observation window and an irradiation window. The image of the volatile phenomenon is shown by irradiating a YAG laser light sheet 2 mm thick from an irradiation window into the anode channel, measurements being made from an observation window with a high spatial resolution video camera (12 bit). The behaviour of vapourized molten carbonates in both the cathode channel inside and the anode channel inside is elucidated under MCFC operating conditions by these experimental devices.

2. Experimental

Fig. 1 shows the photograph of the experimental apparatus, and Fig. 2 shows a schematic diagram of the structure of a cell frame with an observation window and an irradiation window, respectively. The irradiation window is installed on the front of a cell on the gas inlet side, and the observation window is installed on the side of the cell, respectively. The inner diameter of the observation window is 7.6 mm. Therefore, though a conventional cell gas channel is 3.0–4.0 mm in depth, the depth of this cell is 10 mm. In addition, the cell does not use a current collector for visualizing the electrode surface. Moreover, the electrode thickness is half that of a conventional electrode and the electrolyte-loading ratio is conventional for a three-phase interface as the reaction field located near the observation
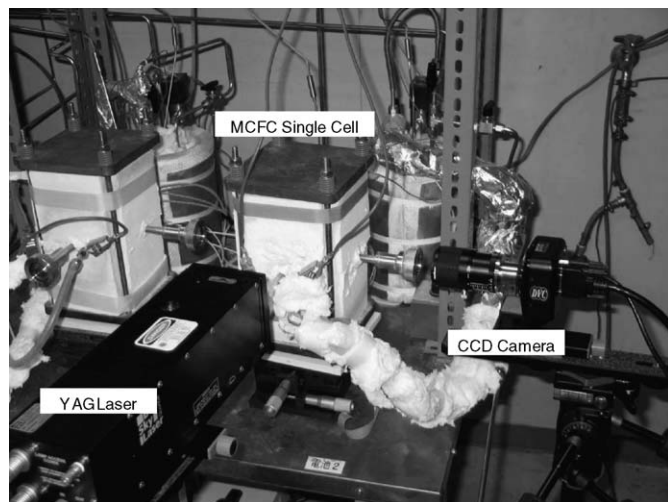

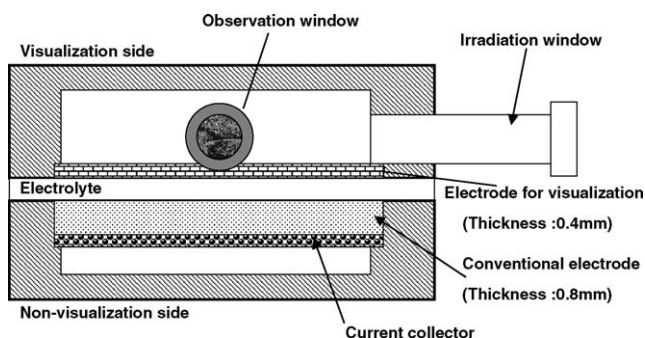Fig. 1. Photograph of experimental apparatus.

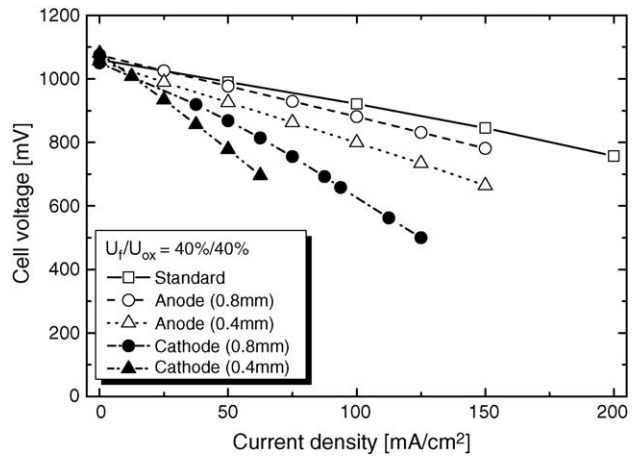Fig. 2. Schematic diagram of MCFC for visualization.

Fig. 3. Initial *V–I* performances of the visualization cells.

window. MCFC components are made by National Institute of Advanced Industrial Science and Technology, Kansai (AIST). Anode and cathode materials are conventional, and the electrolyte is a $(62 + 38)$ mol% $(Li + K)/CO_3$ melt. The electrolyte matrix is lithium aluminium oxide, and the electrode area is 16 cm^2. The fuel cell temperature is controlled by a heater plate to maintain an isothermal state. Anode gas is humidified by its passing the humidifier and is supplied to the MCFC. Cell voltage is measured and recorded by a data logger, and the image of the volatile phenomenon is shown by irradiating a YAG laser light sheet 2 mm thick from an irradiation window into the anode channel, measurements being made from an observation window with a high spatial resolution video camera (12 bit). The image picture of 1300 pixels × 1030 pixels spatial resolution is saved directly into computer memory. In the case of a supply gas condition, the anode standard gas is $70.4H_2/17.6CO_2/12H_2O$, and the cathode standard gas is $70air/30CO_2$ with each gas utilization being 40%.

Fig. 3 shows the initial cell performance used by the experiment under standard conditions (gas composition is each standard gas composition; fuel gas utilization is 40%; oxidant gas utilization is 40%). The *V–I* performance of a cell, which changes the thickness of an anode electrode almost corresponds to conventional cell performance. However, that of a cell, which changes the thickness of the cathode electrode is deteriorated, and there is a strong tendency for the electrode thickness to thin, because there is no current collector in the electrode on the visualization side. Fig. 4 shows the gas composition of anode exhaust gas under OCV conditions. In all visualization cells, if nitrogen concentration in the anode exhaust gas is 1% or less, cross-leakage is not caused and it is determined that all visualization cells can withstand experimentation.

3. Results and discussion

3.1. Electrolyte volatile phenomenon in anode channel

Fig. 5 shows each measurement image in the anode channel when the current density is changed. Here, the anode electrode is located in the lower part of the measurement image, the gas
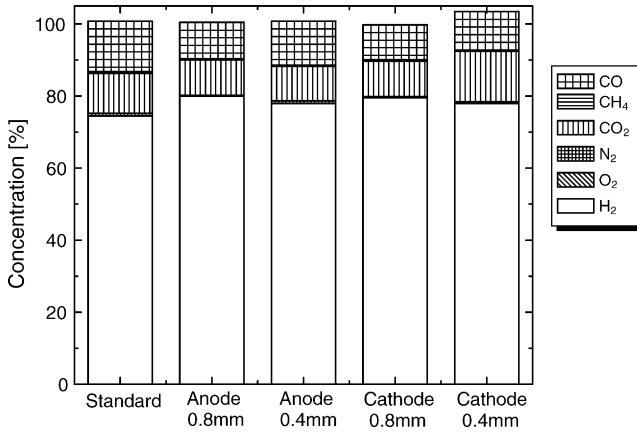
Fig. 4. Gas composition of anode exhaust gas on the visualization cells.

Fig. 6. Effect of current density on KOH concentration.

inlet is located on the left side, and the gas outlet is located on the right side, respectively. Volatile matter is not observed in an anode channel at OCV. However, volatile matter flows in a belt-like manner from the inlet side near the electrode toward the outlet as the current density increases, and its amount increases. Therefore, it is understood that the volatile matter comprises the product materials with a cellular reaction. Volatile matter gathered with a sampling probe for three days are analyzed by ion chromatography. As a result, the composition of the volatile matters is $15Li_2CO_3/85K_2CO_3$ (the result of conversion concentration of Li/K ions into molten salt), and is not an electrolyte ($62Li_2CO_3/38K_2CO_3$). In this instance, product materials with
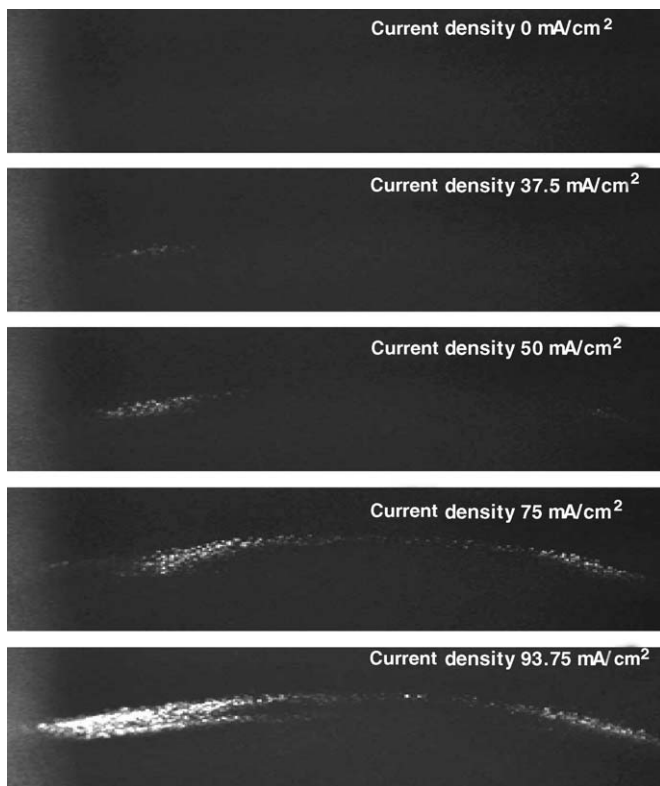

Fig. 5. Measurement image in the anode channel when the current density is changed.

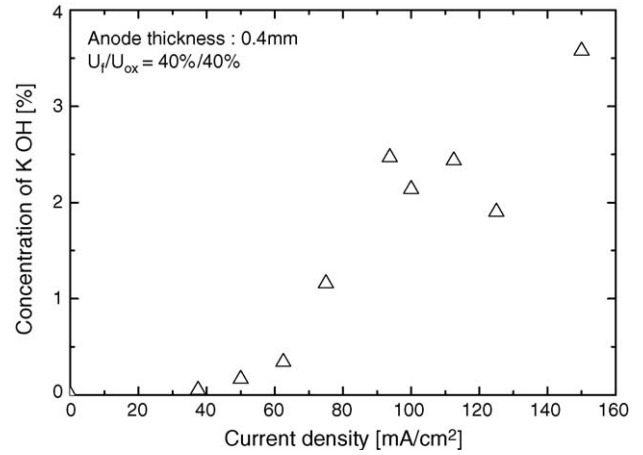a cellular reaction are CO_2 and H_2O; however, CO_2 and H_2O, which are gas-phase under cell temperature conditions, cannot be observed. In addition, because the volatile matter is not under the electrode but is present 2–3 mm from the electrode, it requires time to become an observable solid. Moreover, in experiments using an electrode of a conventional thickness (0.8 mm), volatile matter was not observed at all. It is understood that the volatile matter is generated in accordance with the following procedures from the above-mentioned results. (1) Molten salt volatile matter is KOH generated as the water generated by the cell reaction reacts with an electrolyte. (2) As the generated KOH returns to K_2CO_3 according to Eq. (1) in the region where the concentration rises by the CO_2 generated by the cell reaction, KOH can be visualized as the K_2CO_3 smoke (solid-phase).

$$2KOH + CO_2 \rightarrow K_2CO_3 + H_2O \qquad (1)$$
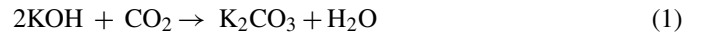
Therefore, the piping blockage is caused by K_2CO_3 adhering to the pipe wall. However, generally, though the KOH concentration to which the molten salt volatilizes is about $10^{-2}\%$ in the calculation from the thermodynamic data [1], the concentration of volatile matter is evaluated by the image processing of these image measurement results.

Here, the each particle in Fig. 5 is defined as a sphere, and the mass of K_2CO_3 is calculated by counting their number, following which the mass of obtained K_2CO_3 is converted into the mass of KOH according to Eq. (1). Moreover, KOH concentration in the anode channel can be defined by dividing the calculated amount of KOH by the volume of the anode channel. The results are shown in Fig. 6. Because the anode-gas-flow-rate is always set to a necessary amount at $150\,\mathrm{mA\,cm^{-2}}$ of the electric current density, an amount of gas greater than a necessary flow rate for the cell reaction is supplied at a low current density. Therefore, the KOH concentration is low at the low current density, and is increased greatly by increasing the current density. The behaviour of this change in concentration corresponds to the results of Fig. 6. The KOH concentration in all experimental results is greater than the calculated values, and is about 3.6% at $150\,\mathrm{mA\,cm^{-2}}$ of the electric current density. It is understood that the cell reaction promotes volatilizing of the KOH. However, as the conventional anode electrode thickness 0.8 mm is twice
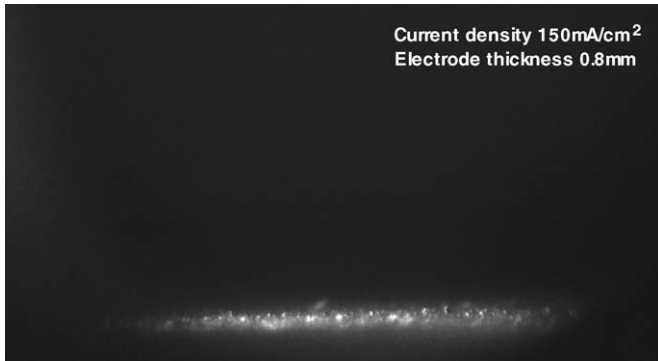
Fig. 7. Measurement image of a conventional anode thickness under 150 mA cm^{-2} of current density.

that of this experiment, the dispersion of the volatile matter to the gas channel is small because it is trapped by an electrode not loaded by electrolytes. Therefore, to prove this assumption, the visualization experiment was done by a conventional electrode thickness (0.8 mm). Fig. 7 shows the measurement image in the anode channel under 150 mA cm^{-2} of the current density. Volatile matter is not observed in the anode channel, and provides the same results by changing the current density. Therefore, our assumption is correct, and it is understood from the current data that a small amount of volatile matter disperses under a conventional anode thickness. Because volatile matter is an extremely small amount, it cannot be observed by this visualization method, and the measurement method is limited by such a small amount.

3.2. Electrolyte volatile phenomenon in cathode channel

Generally, it is recognized that the volatile phenomenon of molten salts in a cathode gas channel is not caused because the cell reaction on the cathode side is the consumption system shown in Eq. (2), and steam, which changes molten salts into hydroxide, is not included in the cathode gas. However, the channel blockage is caused in the heat exchanger installed in cathode outlet by the electrolyte composition. Therefore, the volatile phenomenon of the molten salts in the cathode gas channel is evaluated by the image measurement technique.

$$O_2 + 2CO_2 + 4e^- \rightarrow 2CO_3^{2-} \qquad (2)$$

Fig. 8 shows each measurement image in the cathode channel when the current density is changed. Here, the cathode electrode is located in the lower part of the measurement image, the gas inlet is located on the left side, and the gas outlet is located on the right side, respectively. Volatile matter flows from the inlet side on surface of the electrode. (The distance between volatile matter and the electrode is 0.4 mm) toward the outlet side, and its amount is almost constant for the change in the current density. It is understood that the volatile phenomenon do not depend on a cellular reaction because volatile matter especially flows at OCV. By increasing the current density, volatile matter seems to have decreased a little, and the distance between the electrode and volatile matter seems to become shorter. Therefore, the amount of volatile matters is counted, and the distance of the electrode
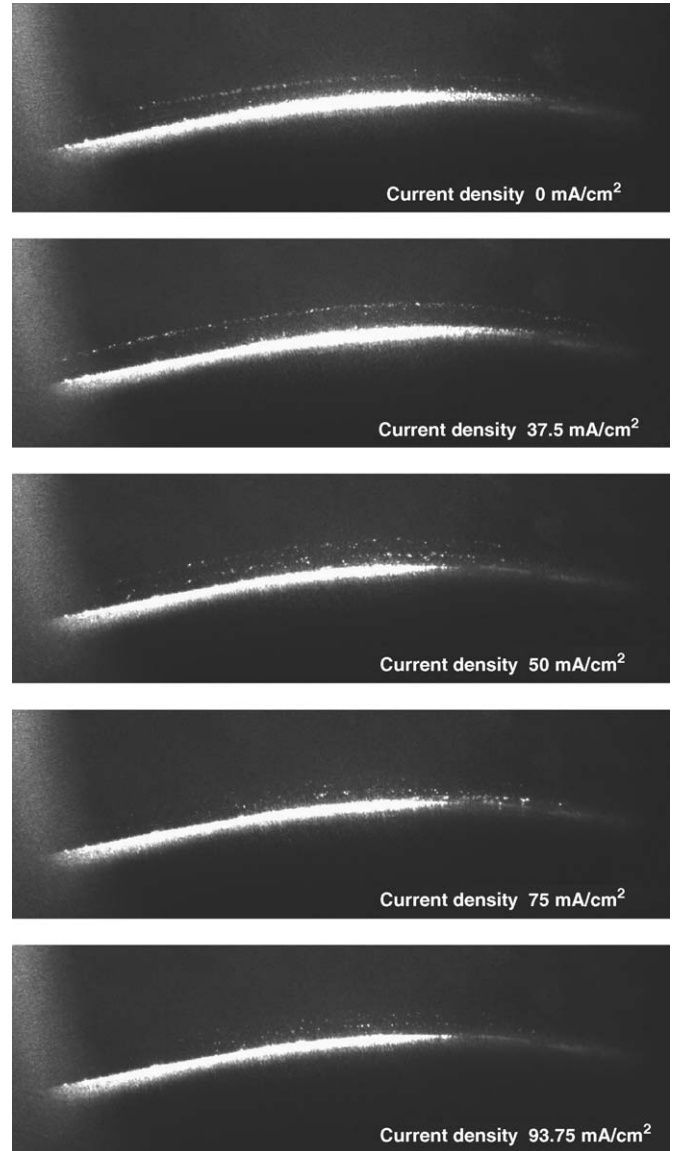

Fig. 8. Measurement image in the cathode channel when the current density is changed.

and volatile matter is measured by image processing. These results are shown in Fig. 9. It is understood that the amount of volatile matter does not depend on the current density. However, the distance between electrode and volatile matter decreases a little by an increase in the current density because the volatile matter is drawn to the electrode by the cathode reaction, which is a consumption reaction. The volatile phenomenon on the cathode side does not have a big change according to the current density like the volatile phenomenon on the anode side. Generally, the electrolyte of the cathode electrode is filled from the matrix up to 60–70% of the electrode thickness toward the channel. However, as the electrode thickness is half (0.4 mm) that of a conventional electrode, there is the possibility that the electrolyte may float on the electrode surface. Therefore, it is understood that because the electrolyte of the cathode surface is sprayed with the supply gas, volatile matter in the cathode channel is molten salt ($62Li_2CO_3/38K_2CO_3$). However, a conventional cathode
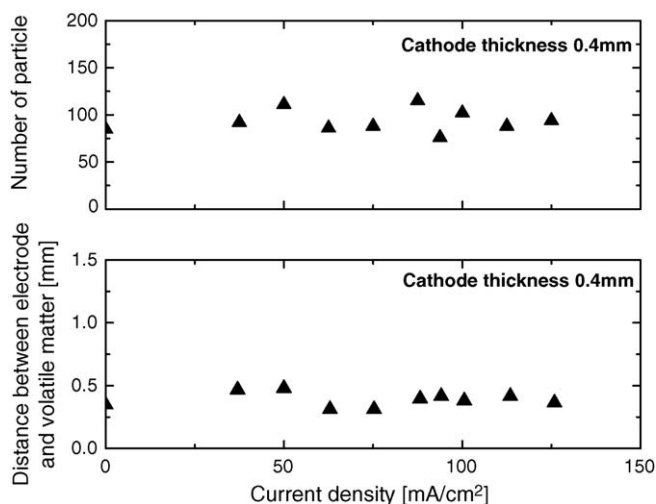
Fig. 9. Effect of cell reaction on volatile matter number and distance between electrode and volatile matter.

Fig. 11. Measurement image of the electrolyte jet from the crack of electrode to the gas channel.

electrode is 0.8 mm thickness and has pores absent electrolytes by 30–40%. Therefore, as the electrolyte does not make contact with gas directly, the electrolyte is not sprayed with the supply gas. Therefore, visualization experiments were done with a conventional electrode thickness (0.8 mm) to prove this assumption. Fig. 10 shows the measurement image in the cathode channel under OCV conditions. Here, because the upheaving electrode is irradiated by a laser beam, the upstream part of the electrode is shining. It is confirmed by changing the irradiation direction of the laser sheet and a measurement interval of CCD camera that the shining part is not volatile matter. Volatile matter is not observed on the cathode surface, and the same results are obtained by changing the current density. Therefore, our assumption is correct, and it is understood that molten salt is not sprayed with the conventional thickness of a cathode. However, there is a possibility of dispersion of the molten salts from a wet seal part where the electrolyte makes direct contact with gas. Moreover, these volatile matters could not be identified by ion chromatography because an amount of the sample necessary for the analysis was not able to be obtained by which volatile matters were captured to the wall of the sampling probe, etc. Therefore, these volatile matters on the cathode electrode surface should be analyzed by re-examining the method of gathering these volatile matters.

From a different perspective, the surface of the cathode electrode becomes curved because the cathode electrode is softer than the anode electrode, and the curvature of the electrode
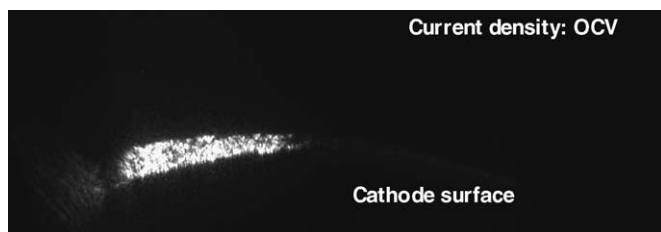
grows as the number of operating hours passes. Finally, the curvature of the electrode cracks and the electrolyte jets from the crack to the gas channel as shown in Fig. 11. This electrolyte jets intermittently and there is a small decrease with an increase in the current density. Though the reason is not yet certain, it is understood that the electrolyte loss is promoted if cross-leakage is caused. Therefore, it is important from not only from the standpoint of improved performance of the current collector, but also from the standpoint of electrolyte volatilization, that a current collector be installed to prevent the electrode from cracking. Moreover, if the electrolyte is filled more than usual for extended operation, such phenomena will be caused, and the piping and the gas channel of heat exchanger will be blocked.

4. Conclusion

The objective of this study is to evaluate volatile behaviour of molten salt in a DIR-MCFC by the image measurement technique. The obtained results in this study are summarized as follows.

(1) *In the anode volatilization phenomenon:* Molten salt volatile matter is KOH generated as the water generated by the cell reaction reacts with the electrolyte, and as the generated KOH returns to K_2CO_3 in the region where the concentration rises by the CO_2 generated by the cell reaction. Moreover, the catalyst pollution in DIR-MCFC is caused by the K_2CO_3's adhering to the catalyst.

(2) *In cathode volatile phenomenon:* The possibility of volatile matter, which is molten salt ($62Li_2CO_3/38K_2CO_3$), is high. If the electrolyte is filled more than usual for extended operation, these phenomena will occur and the piping and the gas channel of heat exchanger will be blocked.

(3) If the cross-leakage is caused, the electrolyte gushes from the cracking electrode section, and the electrolyte loss is accelerated.

(4) It is important not only in terms of improved current collector performance, but also from the standpoint of electrolyte volatilization, that a current collector be installed to prevent the electrode from cracking.

References

[1] C. Hirai, M. Matsumura, S. Tanaka, Studies on reforming catalyst for internal reforming molten carbonate fuel cell, Abstract Book of Denchi-Touron-kai, The 29th Battery Symposium, Japan, pp. 79–80, 1988.

[2] K. Sugiura, K. Ohtake, Deterioration of a catalyst's activity by liquid-phase MC poisoning in DIR-MCFC, J. Chem. Eng. Jpn. 21 (6) (1995) 1170–1178.

Fig. 10. Measurement image of a conventional cathode thickness under $150\,\mathrm{mA\,cm^{-2}}$ of current density.

[3] Y. Miyake, N. Nakanishi, T. Nakajima, Y. Itoh, T. Saitoh, A. Saiai, H. Yanaru, A study on degradation phenomena of reforming catalyst in DIR-MCFC, J. Chem. Eng. Jpn. 21 (6) (1995) 1104–1109.

[4] K. Sugiura, I. Naruse, K. Ohtake, Deterioration of a catalyst's activity in direct internal reforming-molten carbonate fuel cells (effect of adsorption of vapour-phase molten carbonate), J. Jpn. Soc. Mech. Eng., Ser. B 65 (629) (1999) 330–336.

[5] K. Sugiura, M. Yamauchi, K. Tanimoto, Y. Yoshitani, Evaluation of volatile behaviour and the volatilization volume of molten salt in DIR-MCFC by using the image measurement technique, J. Power Sources 145 (2005) 199–205.